RSC Advances

ROYAL SOCIETY OF CHEMISTRY

www.rsc.org/advances

RSC Advances

RSCPublishing

COMMUNICATION

Sulfur-doped-ZnO-nanospire-based Transparent Flexible Nanogenerator Self-powered by Environmental Vibration

Cite this: DOI: 10.1039/xoxxoooooox

Received
Accepted

DOI:

www.rsc.org/ees

Cheng-Liang Hsu,*[a] I-Long Su[a] and Ting-Jen Hsueh*[b]

An S-doped-ZnO-nanospire-based nanogenerator that converts environmental vibration into electrical energy is proposed. The nanogenerator piezoelectricity is improved by loading weight, ultraviolet (UV), and a sharp Pt/ZnO nanowire electrode. The output current and voltage of nanogenerator in the dark and under UV light are ~4.32×10^{-8}A and ~0.646V and 5.73×10^{-8}A and ~0.689V.

1. Introduction

Harvesting energy from the environment has attracted great interest. Energy resources include light, wind, thermal energy, mechanical vibration, and body movement.[1] Harvesting such sources is important for long-term sustainable development. Portable and wearable electronics have gained increasingly complex functions and decreased in size. Because battery size is difficult to reduce, self-powered devices have attracted attention. Various energy harvesting approaches have been developed for self-powered devices, including those based on electromagnetic,[2] solar cell,[3] triboelectric,[4] pyroelectric,[5] and piezoelectric harvesters.[6] Among these, piezoelectric harvesters effectively harvest mechanical vibration and body movement energy. Piezoelectric harvesters can be made of single-crystal (e.g., quartz, $LiNbO_3$, $LiTaO_3$, KNbO),[7] bulk ceramic (e.g., PZT, BT),[8] thin film (e.g., AlN, InN, ZnO),[9] and polymer (e.g., PVDF)[10] materials. The impedance and permittivity of ZnO is lowest among these materials, and its high conductivity allows high output current.

ZnO nanowires (NWs) have been widely applied in triboelectric, pyroelectric, and solar harvesters and piezoelectric nanogenerators (NGs).[3-6] The performance of ZnO-NW-based piezoelectric NGs has been improved using approaches such as doping[11] and the use of suitable electrode materials[12] and flexible substrates.[13-29] Dopants can change the intrinsic properties of ZnO, making it n-or p-type. Contact electrode materials affect the energy level of the Schottky barrier height (SBH), which influences piezoelectric characteristics. Because the mechanical resistance of flexible substrates (e.g., those made of paper, plastic fibers, thin metal foil, or polymers)[13-29] is lower than that of hard substrates (e.g., those made of Si, glass, or sapphire), the deformation of flexible substrates is usually larger than that of hard substrates for a given compression or tensile strain force. Our previous work reported that the performance of ZnO-NW-based NGs is improved by a flexible polyethylene terephthalate (PET) substrate.[13] In the present investigation, sulfur (S)-doped ZnO (ZnO:S) NWs were synthesized on a PET substrate. The doping increased the conductivity of piezoelectric NGs. A rectangular region was cut in the center portion of the electrode substrate to enhance deformation. The results show that ZnO:S-NW-based piezoelectric NGs can output energy converted from environmental vibration. Increased weight stress and ultraviolet (UV) light illumination improved the piezoelectric properties of ZnO:S-NW-based piezoelectric NGs.

2. Experimental Section

PET is a transparent and chemically stable material, but it becomes weak at high temperatures. In general, the operating temperature of the hydrothermal method does not exceed 100 °C, making it suitable for PET substrates. Al-doped ZnO (AZO) thin film as a seed layer was deposited on a PET substrate via radio-frequency sputtering. ZnO:S NSs were synthesized on the AZO seed layer via the hydrothermal method in a sealed chamber heated to 99°C for 6 hours. The reagents were 0.06 M hexamethylenetetramine (HMTA, $C_6H_{12}N_4$) and 0.06 M zinc nitrate hexahydrate ($Zn(NO_3)_2{\cdot}6H_2O$) with 0.002 M (sample A) or 0.01 M (sample B) thiourea (CH_4N_2S). HMTA and zinc nitrate hexahydrate were the growth sources of synthesized ZnO NWs. Thiourea was the S dopant source. The nanostructured contact electrode was 20-nm-thick platinum (Pt) coated on a ZnO NWs/PET sample via direct-current sputtering. A rectangular hole (0.6 cm × 1.4 cm) was cut out in the center of the Pt/ZnO NWs/PET substrate to enhance deformation. The piezoelectric NG was assembled from a ZnO:S NW sample and a Pt/ZnO NWs/PET substrate combination with hot-melt adhesive. Similar growth and processing steps were reported in a previous study.[13]

Figures 1(a) and **1(b)** show a photograph and a schematic of the cross-section structure of the piezoelectric NG, respectively. The environmental vibration source was a table in our laboratory. Environmental vibrations are mostly low-frequency vibrations. The piezoelectric NG samples were placed on a

table to absorb and convert environmental vibration energy. The crystallinity, optical properties, and doping concentration were measured with scanning electron microscopy (SEM), transmission electron microscopy (TEM), X-ray diffraction (XRD), and photoluminescence (PL) spectroscopy. These measurement tools are same as previously reported.[13] The current-voltage (*I-V*) curves were measured by Keithley 4200. The output piezoelectric current and voltage were measured using Stanford SR570 low-noise current and SR560 low-noise voltage amplifiers.

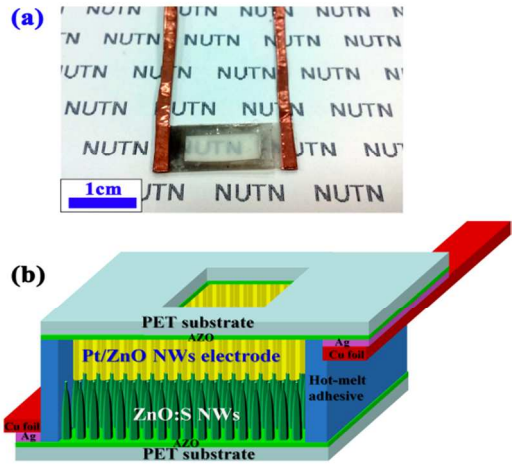

Fig. 1 (a) Photograph and **(b)** schematic structure diagram of piezoelectric NG.

3. Results and discussion

Figures 2(a) and **2(b)** show cross-section SEM images of samples A and B, respectively. The ZnO:S NWs grew uniformly on the PET substrate. The S dopant concentrations in sample A (0.002 M CH_4N_2S) and sample B (0.01 M CH_4N_2S) were 1.06 and 2.03 at.%, respectively, as obtained from energy-dispersive X-ray spectroscopy (EDS) analysis. Compared to previously reported work[30-31] on undoped ZnO NWs, the morphology of ZnO:S NWs has been changed from NWs to nanospires (NSs) by increased S dopants. The tops of the doped NWs were needle-shaped. The tip length increased with increasing S concentration.

Figures 2(c) and **(d)** show 2θ-scan XRD patterns and room-temperature PL spectra of undoped and ZnO:S NS samples, respectively. The XRD peaks of the ZnO:S samples correspond to a wurtzite crystal structure and shift to smaller angles with increasing S concentration. The PL spectra show that the green emission peak of ZnO:S samples was blue-shifted and increased with increasing S content. The PL peak of oxygen vacancies in ZnO is around the green emission position, and thus the results indicate that the S dopant increased the quantity of oxygen vacancies.

Figures 3(a) and **3(b)** show a TEM image, EDS element mapping, high-resolution TEM image, and selected area electron diffraction (SAED) pattern of ZnO:S NSs. Based on the TEM image and Zn and O element mapping, Zn and O were the main elements. The S spot signal was uniformly distributed over the NSs. The SAED pattern of ZnO:S NSs indicates a wurtzite crystal structure. The high-resolution TEM image shows a single crystal with no observed defects.

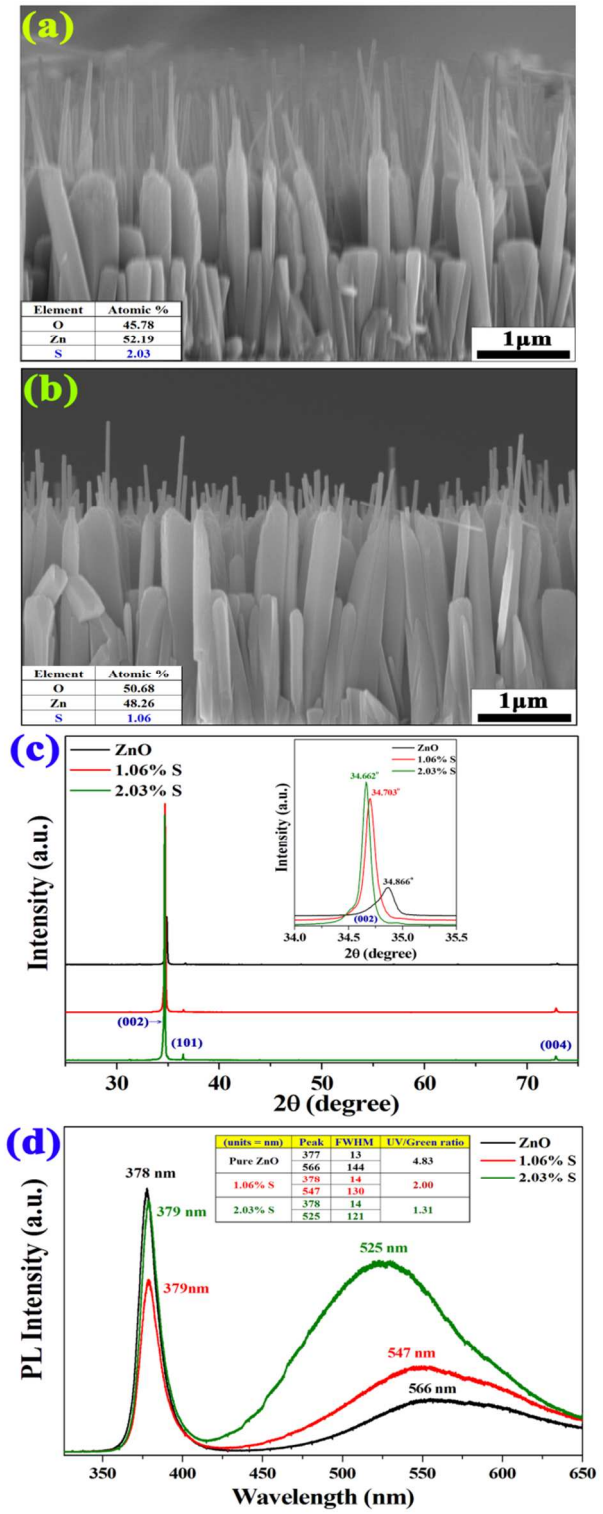

Fig. 2 Cross-sectional SEM images of **(a)** sample A and **(b)** sample B, revealing uniform ZnO:S NWs. **(c)** 2θ-scan XRD patterns and **(d)** PL spectra of pure and S-doped ZnO NWs.

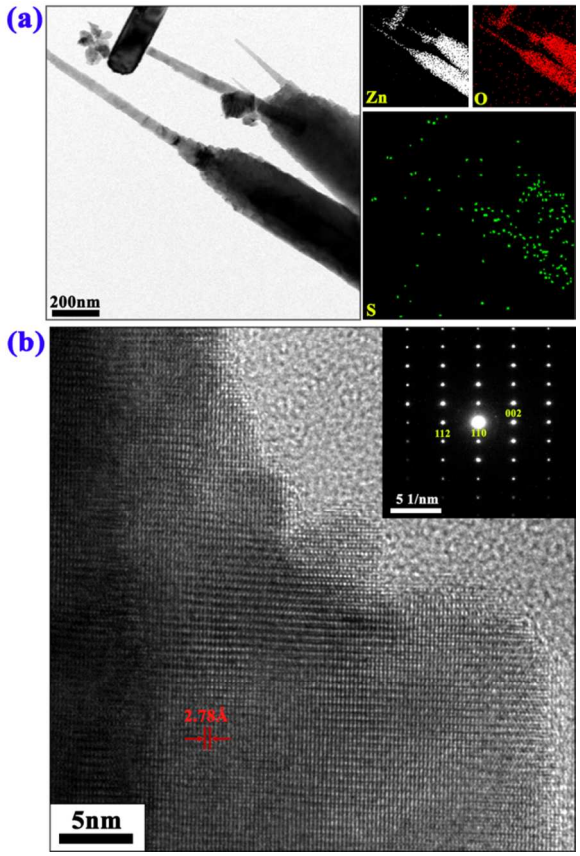

Fig. 3 (a) TEM image and corresponding Zn, O, and S EDS mapping images. **(b)** High-resolution TEM image and SAED pattern of ZnO:S NW.

Figure 4(a) depicts *I-V* curves of the piezoelectric NG measured under a loading weight force and UV light exposure. **Figures 4(b)** and **4(c)** shows *I-V* curves of piezoelectric NGs based on pure ZnO NWs and ZnO:S NSs with and without a loading weight force (12.5 g/cm^2) and UV light exposure measured at a relative humidity of 45%. These *I*−*V* curves correspond to the Schottky junction properties. The dark current and UV photocurrent of the ZnO NW and ZnO:S NS samples slight increased with a weight force (12.5 g/cm^2). When weight was applied, the distance between the ZnO:S NSs and Pt/ZnO NWs slightly decreased, increasing the contact area and thus the conductivity current. The UV photocurrent of the piezoelectric NGs based on ZnO NWs and ZnO:S NSs are larger than dark current ~2.01 and ~2.84 times without loading weight force. These photocurrent gains of the piezoelectric NG are smaller than previously reported values for photodetectors with a small UV light source (wavelength 365nm, power density 0.25 mW/cm^2) and UV light almost absorbed by the PET substrate.[30] The dark current (4.86×10^{-8}A) of the ZnO:S-NS-based piezoelectric NG was larger than that of the NG based on ZnO NWs (8.29×10^{-9}A) by ~5.86 times under a 10-V bias, indicating that the S dopant reduced that resistance of the ZnO:S NS sample.

Figures 5(a) and **5(b)** show the output piezoelectric current of piezoelectric NGs based on ZnO NWs and ZnO:S NSs with and without a loading weight force in the dark and under UV exposure. The output piezoelectric currents were produced by the NG devices converting environmental vibration energy. The piezoelectric currents increased with increasing loading weight. These NG devices were isolated vibration energy transmission from table by placed NG devices above glass or expandable polystyrene (EPS) substrate, which act isolation layer and absorbs partial environmental vibration energy. EPS is softer than glass and absorbs most vibration energy, decreasing the output piezoelectric current. EPS and glass were used to verify that the output current of the piezoelectric NG was from the conversion of environmental vibration.

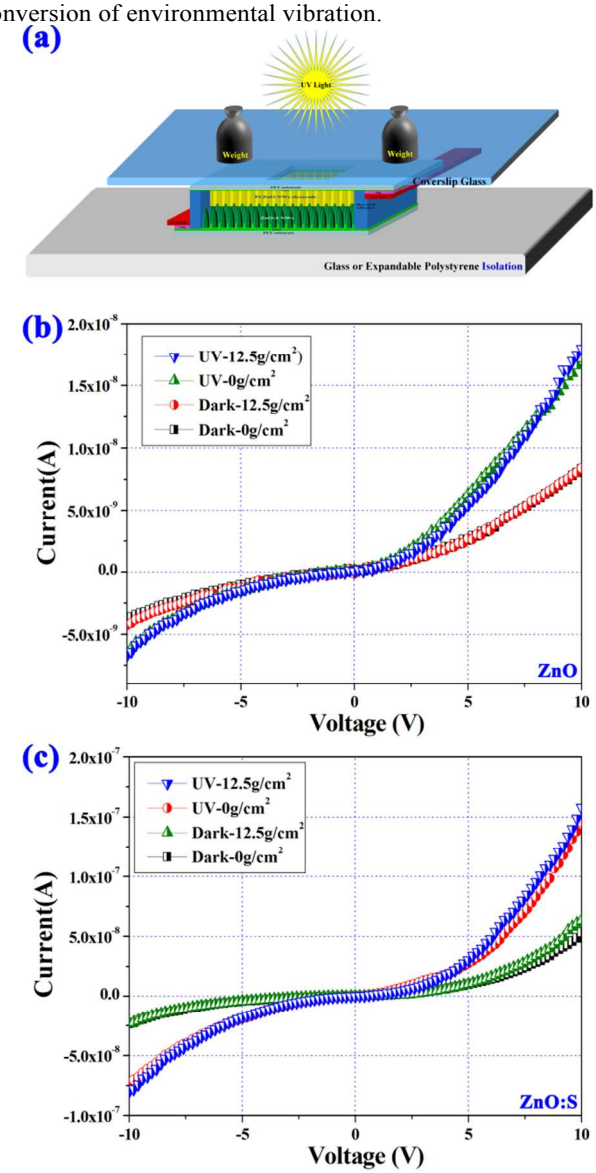

Fig. 4 (a) Piezoelectric measurement environment. *I-V* curves of NGs based on **(b)** pure ZnO NWs and **(c)** ZnO:S NSs with and without weight force and UV light exposure.

In the dark without vibration isolation, the highest output piezoelectric current was ~4.32×10^{-8} A for the ZnO:S-NS-based NG device, slightly higher than that of the ZnO-NW-based NG (~4.14×10^{-8} A) around 4.3% under loading weight 500 g/cm^2 force. The lowest output current of the ZnO-NW-based NG was ~1.0×10^{-8} A under 0 g/cm^2 force in the dark. This result is higher a previously reported value (5×10^{-10} A) for converting electrical energy from environmental vibration,[13] indicating that the rectangular hole enhanced NG structure deformation. Under UV illumination and a 500 g/cm^2 force, the highest output piezoelectric current was 5.73×10^{-8} A for the ZnO:S-NS-based NG device, larger than that for the ZnO-NW-based NG (4.97×10^{-8} A) around 15.3% without any vibration isolation

layer. The output piezoelectric current of NGs based on ZnO NWs and ZnO:S NSs increased by 20.2% and 32.6% under UV exposure. These output piezoelectric currents were increase slower and toward saturation when weight forces over 50 g/cm^2. According to our experiences, the measurement safe range is preferably less than 500g/cm^2, due to these NG samples were stable outputted electrical power for a long time under weight force < 500g/cm^2.

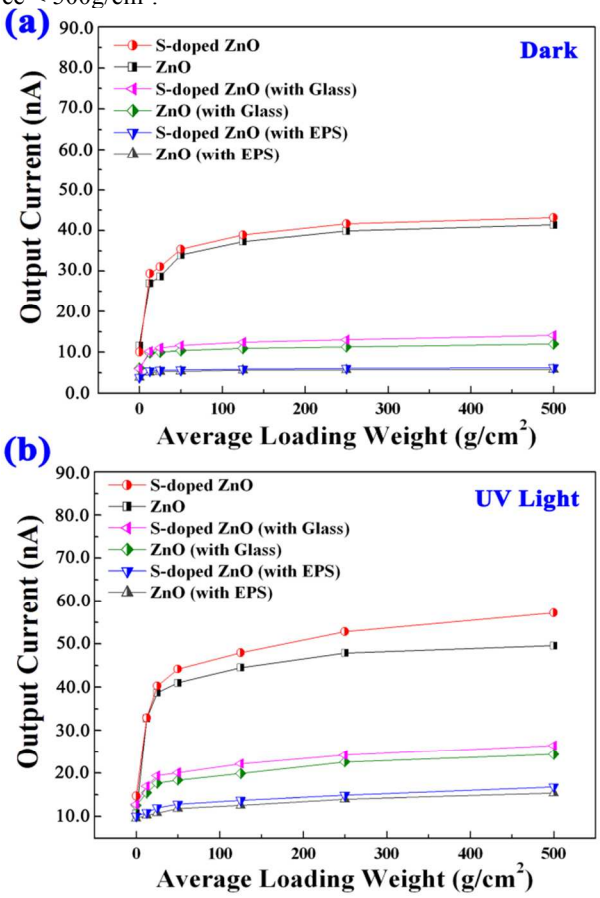

Fig. 5 Output current NGs based on ZnO NWs and ZnO:S NSs with various weight forces **(a)** in the dark and **(b)** under UV exposure.

Figures 6(a) and **6(b)** show the output piezoelectric voltage of piezoelectric NGs based on ZnO NWs and ZnO:S NSs with loading various weight forces in the dark and under UV exposure. The output voltages were converted from environmental vibration energy and increased with increasing weight force. The EPS and glass isolation layer reduced the output voltage. Without the isolation layer, the highest output piezoelectric voltage was ~0.646 V for the ZnO:S-NS-based NG, higher than that for the ZnO-NW-based NG (~0.586 V) around 10.2% under loading weight 500 g/cm^2 force in the dark. Under UV illumination and a 500 g/cm^2 force, the highest output piezoelectric voltage was ~0.689 V for the ZnO:S-NS-based NG, slightly larger than that for the ZnO-NW-based NG (~0.659 V) around 4.6% without any vibration isolation layer. The highest output power values for the ZnO:S-NS- (dark: 2.4 nW, UV: 3.9 nW) and ZnO-NW-based NGs (dark: 1.8 nW, UV: 3.2 nW) were obtained without a weight force. Under a 500 g/cm^2 force, the highest output power values for the ZnO:S-NS- (dark: 27.9 nW) and ZnO-NW-based NGs (dark: 24.2 nW) were 39.5 and 32.8 nW under UV exposure, respectively. The output power increased around 10-fold when the loading weight was ≥ 12.5 g/cm^2. The output power of NGs based on ZnO:S NSs and ZnO NWs increased by 41.5% and 35.5% under UV illumination, respectively.

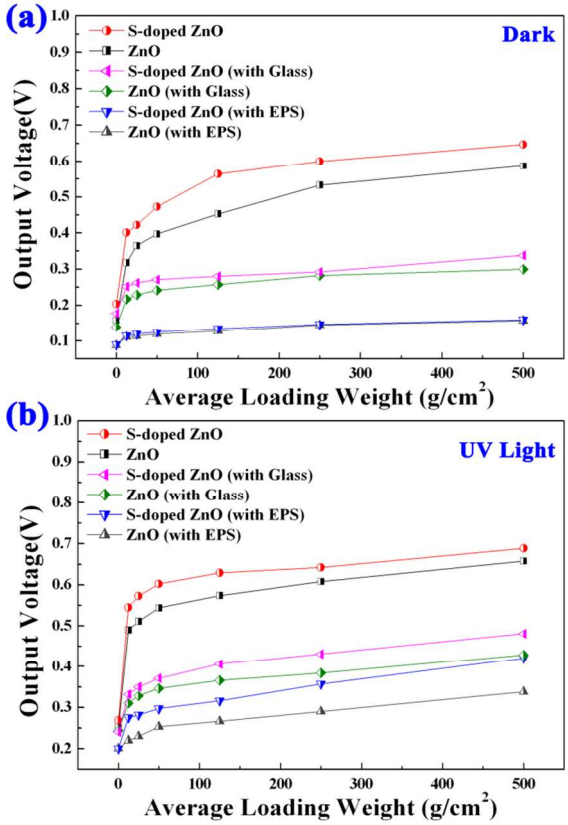

Fig. 6 Output voltage of NGs based on ZnO NWs and ZnO:S NSs with various weight forces **(a)** in the dark and **(b)** under UV light.

The filter function of the measurement equipment was used to measure the ZnO:S-NS-based NG. The output current signal of the ZnO:S-NS-based NG was filtered to > 1 kHz and < 1 kHz regions, as shown in **Figure 7(a)**. These current signals increased ~3-fold when a 12.5 g/cm^2 force was applied. The frequency of the output current signal has a significant correlation with environmental vibration frequency, and thus the current of the < 1 kHz signal is larger than that of the > 1 kHz signal, which means that environmental vibration frequency is lower than 1 kHz. To further analyze the < 1 kHz output current signal region, it was filtered into smaller sections: 1~3 Hz, 3~10 Hz, 10~30 Hz, 30~100 Hz, 100~300 Hz, and 300 Hz~1 kHz. **Figure 7(b)** shows the filtered frequency sections of the output current signals of NG based on ZnO:S NSs. The highest output current in each frequency section is shown in **Figue 7(c).** These output current signals at various frequencies are similar to sine waves, and thus may have been affected by the Fourier transform of the filter. The 30~100 Hz frequency section had the highest output current. The voltage and frequency of our laboratory electrical power (standard electricity output in Taiwan) are *AC*-110 V and 60 Hz, respectively. In general, the frequency of machinery vibration is correlated with the electrical power frequency. The highest output current at 30~100Hz was assumed to be generated by laboratory machinery vibration. These results are consistency with corresponding to ZnO:S NSs NG devices transferred electrical energy from environmental vibrations.

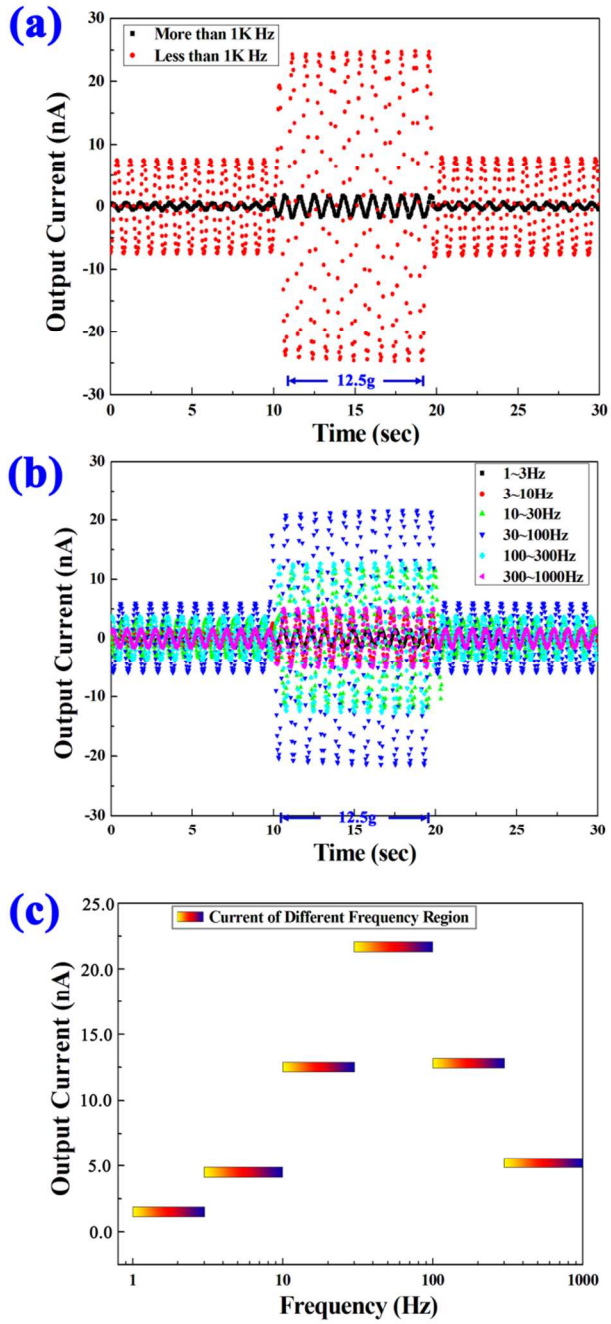

Fig. 7 (a) Output current signal of ZnO:S-NS-based NG filtered to > 1 kHz and < 1 kHz regions. **(b)** < 1 kHz frequency of output current signal have been smaller section analysis, which maximum output current were picked up and described in **7(c)**.

Figures 8(a) and **8(b)** show a common electrode plate and the proposed Pt/ZnO NWs/PET substrate on ZnO nanostructures, respectively. **Figures 8(a)** and **8(b)** show a common electrode plate and the proposed Pt/ZnO NWs/PET substrate on ZnO nanostructures, respectively. Although the ZnO:S NSs and ZnO NWs are uniform growth on PET substrate by SEM observed, but it is difficult to prevent growth few, ultra-long ZnO:S NSs or ZnO NWs. These few ultra-long ZnO:S NSs are major outputted power source due to touch and sustain Pt/ZnO NWs electrode. Based on past AFM measurement reports, the single ZnO NW produced 10~100 pA piezoelectric current with various force.[6, 32] In this study, there are billions of ZnO:S NSs on substrate and expected that piezoelectric current larger than mA region, but these NG only generated a small current ~43 nA. Calculated the current ratio, the ultra-long ZnO NSs are around ~10^5 wires. Compared with the deformation of the common electrode plate, that of the proposed electrode substrate was enhanced by the rectangular hole. The modified electrode substrate is more sensitive to environmental vibration and produces more electrical energy. When applied loading weight, the smaller electrode size was suffered higher stress force.

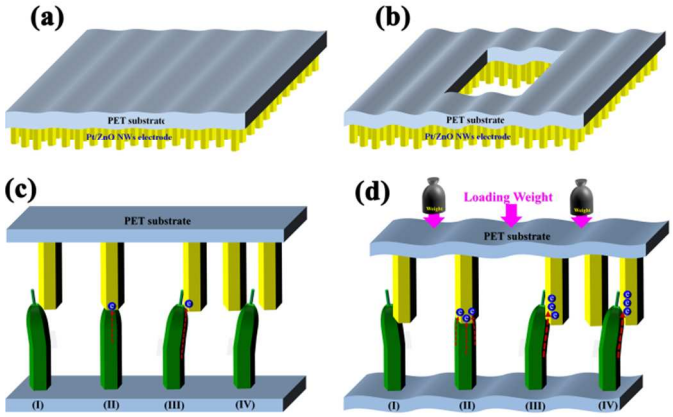

Fig. 8 (a) Common electrode plate and **(b)** proposed Pt/ZnO NWs/PET substrate on ZnO nanostructures. Schematic illustration of piezoelectric electrons of ZnO:S-NW-based NG **(c)** without and **(d)** with applied loading weight force.

Figures 8(c) and **8(d)** show the piezoelectric current four types of ZnO:S-NS-based NG without and with an applied weight force, respectively. The electron flows and piezoelectric potential increased with increasing applied force. The positive potential (V^+) and negative potential (V^-) are generated on the tensile and compression sides of ZnO:S NSs, respectively.[21] The Schottky barrier contact formed between ZnO NWs and Pt/NW electrode interface, as shown in Fig. 4. In Fig. 8(c), the type II and III generates electrons flows from ZnO:S NSs to Pt/ZnO NW electrode, due to the Pt/ZnO NW electrode contacted on the compression side of ZnO:S NSs. Compared with Fig. 8(c), the type II, III, and VI in Fig. 8(d) produced more electrons with applied weight force due to the distance between ZnO:S NSs and the electrodes being shortened and the force on NSs to cause more compression. The contact between ZnO:S NSs and Pt/NW electrodes increased with decreasing distance. The ZnO:S NSs will be contact to two or more Pt/NWs electrodes, which has more opportunities to contact the compression side of ZnO:S NSs, such as Fig.8 type VI. Under a 500 g/cm^2 force, the output current and voltage of the ZnO:S-NS-based NG increased by ~32.6% and ~6.6% under UV exposure, respectively. According past reports,[33-34] the output current and voltage of ZnO NG was decreased significantly by UV irradiation (100W and 2W/cm^2). Their AlN/sapphire and sapphire substrate are high UV light transmittance ~70%. In this study, the handheld UV (365nm) power density is only 0.25mW/cm^2, which is much lower than previous reports 3~4 orders of magnitude intensity. UV transmittance of the Pt/ZnO NWs electrode is only 1.41%. The weak UV irradiation was very slight to exposure on NSs and electrode interface. Thermometer was measured that surface temperature of NG was increased 3~5°C under UV exposure. Because of handheld UV lamp (~50°C) was near to NG position, and caused that NG temperature increase due to absorption and associated heating. Thermal expansion (coefficient: 40~80 μm/K) of PET substrate

induces the NG structure deformation and then increase output power performance.

In general, the piezoelectric coefficient (d_{33}) of ZnO can be presented as $d_{33} = 2P_s\varepsilon_0\varepsilon_r Q_{eff}$,[35] where P_s denotes spontaneous polarization, ε_0 denotes permittivity of free space, ε_r denotes relative permittivity and Q_{eff} denotes effective electrostriction coefficient. The P_s and ε_r have been adjusted and increased with dopant,[36] which enhance the d_{33} performance. The Young's modulus values of PET and ZnO are 2~2.7 and 114.6~217.5 GPa, respectively (PET is much softer than ZnO). When applied loading weight in ZnO:S NSs NG, the deformation ratio of PET substrate was larger than ZnO:S NSs or ZnO NW, which means that a lot part force be absorbed by PET substrate and caused nano size deformation on surface of PET, as shown in Fig. 8(d).

Figure 9(a) and **9(b)** show interface band diagrams of ZnO NW and ZnO:S NS with Pt electrode. The ZnO/Pt and ZnO:S NS/Pt electrode interface are a Schottky barrier contact. Compression and tensile strain change the Schottky barrier height, and conduction band (E_c) and valence band (E_v) curves due to the piezoelectric materials property.[37]

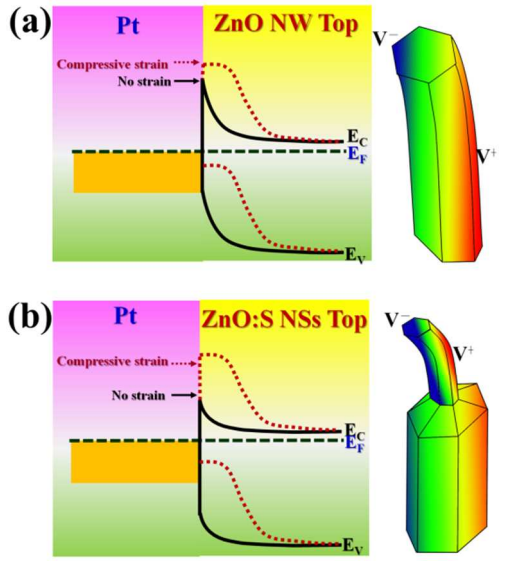

Fig. 9 Band diagrams of **(a)** ZnO NW/Pt and **(b)** ZnO:S NS/Pt interface.

According the previous reports, the n-type doping will increase the electron concentration and cause screening effect,[38] which reduces the piezoelectric potential of ZnO NG. In this study, the S dopant has changed that morphology of ZnO NWs and formed ZnO:S NSs. The tops of ZnO:S NSs were needle-shaped, which diameter is smaller than ZnO NWs around 5~7 times. Under the same strain force, the deformation of ZnO:S NSs tip is greater than ZnO NWs and compensate for the loss piezoelectric potential of screening effect. The small diameter of ZnO:S NSs top cause that contact area of ZnO:S and Pt electrode are substantially reduced. The slight environmental vibration energy will transfer to make these ZnO:S NSs constantly shaking in small size. The small moving of ZnO:S NSs continuity change the contact position of Pt/ZnO NWs electrode and produce great amount electrons. The energy of environmental vibration deformed the PET surface, increasing the internal stress of the PET substrate. The ZnO:S NSs NG produce more piezoelectric power and is more sensitive to environmental vibration. Previous reported flexible ZnO-nanostructure-based NGs are compared with the proposed NG in **Table 1**. In past reports, these applied force energy were used ultrasonic power, human finger and bending machine. In this study, the vibration energy is not using any applied force from machine or human, it is only supplied by laboratory environmental vibration.

4. Conclusions

High-density, vertical ZnO:S NSs were uniformly synthesized on a PET substrate via the hydrothermal method. The S dopant (2.03 at.%) was uniformly distributed over the NSs. A rectangular hole was cut in the center of the Pt/ZnO NWs/PET electrode to enhance the deformation of the NG. Under a loading weight of 500 g/cm^2, the ZnO:S-NS-based piezoelectric NG had an output current of ~4.32×10^{-8} A and a voltage of ~0.646 V in the dark by converting environmental vibration. Under UV illumination and a weight of 500 g/cm^2, the highest output current and voltage of the ZnO:S-NS-based NG were 5.73×10^{-8} A and ~0.689 V, respectively. Based on filter function analysis, the highest response current was obtained at 30~100 Hz, which is assumed to be generated by laboratory machinery vibration. A ZnO:S-NS-based NG with large output current and voltage was thus obtained.

Acknowledgments

The authors would like to thank the Ministry of Science and Technology, Taiwan, for financially supporting this research under Contract No. MOST 103-2221-E-024-016-

Notes and references

[a] Department of Electrical Engineering, National University of Tainan, Tainan 700, Taiwan, ROC. Fax: +886-6-2602305; Tel: +886-6-2606123#7785; E-mail: clhsu@mail.nutn.edu.tw

b National Nano Device Laboratories, Tainan 741, Taiwan, ROC; E-mail: tingjen1123@yahoo.com.tw

1. Z. G. Yang, J. L. Zhang, M. C. W. Kintner-Meyer, X. C. Lu, D. W. Choi, J. P. Lemmon, J. Liu, *Chem. Rev.* 2011, **111**, 3577.
2. O. Zorlu, E. T. Topal, H. Kulah, *IEEE Sens. J.* 2011, **11**, 481.
3. M. Law, L. E. Greene, J. C. Johnson, R. Saykally, P. D. Yang, *Nat. Mater.* 2005, **4**, 455.
4. F. R. Fan, Z. Q. Tian, Z. L. Wang, *Nano Energy*, 2012, **1**, 328.
5. R. W. Whatmore, *Rep. Prog. Phys.* 1986, **49**, 1335.
6. Z. L. Wang, J. H. Song, *Science*, 2006, **312**, 242.
7. Y. Wang, Y. J. Jiang, *Opt. Mater.* 2003, **23**, 403.
8. F. Xia, X. Yao, *J. Mater. Sci.* 1999, **34**, 3341.
9. F. Bernardini, V. Fiorentini, D. Vanderbilt, *Phys. Rev. B*, 1997, **56**, 10024.
10. B. Mohammadi, A. A. Yousefi, S. M. Bellah, *Polym. Test*, 2007, **26**, 42.
11. N. A. Spaldin, *Phys. Rev. B*, 2004, **69**, 125201.
12. Y. H. Ko, S. H. Lee, J. S. Yu, *Appl. Phys. Lett.* 2013, **103**, 022911.
13. C. L. Hsu, K. C. Chen, *J. Phys. Chem. C*, 2012, **116**, 9351.
14. B. Saravanakumar, S. J. Kim, *J. Phys. Chem. C*, 2012, **118**, 8831.
15. Y. Qiu, J. X. Lei, D. C. Yang, B. Yin, H. Q. Zhang, J. M. Bian, J. Y. Ji, Y. H. Liu, Y. Zhao, Y. M. Luo, L. Z. Hu, *Appl. Phys. Lett.* 2014, **104**, 113903.
16. M. Song, Y. Zhang, M. Z. Peng, J. Y. Zhai, *Nano Energy*, 2014, **6**, 66.
17. M. Lee, J. Bae, J. Lee, C. S. Lee, S. Hong, Z. L. Wang, *Energy Environ. Sci.* 2011, **4**, 3359.

Tab. 1 Applied force and measured output electrical results of various flexible ZnO-nanostructure-based NGs.

ZnO Morphology	Nano Size	Applied Force	Output Voltage	Output Current	Output Power	Substrate	Ref.
S-doped nanospires	Diameter = 20~200nm, Length = 4~5um	**Environmental vibration**	0.646V	43.2nA	27.9nW	PET	This work
Nanowires	Diameter = ~100nm, Length = ~1um	**Environmental vibration**	0.586V	41.4nA	24.3nW	PET	This work
Nanowires	Diameter = ~100nm, Length = ~1um	2% bending		2.5nA		PET	[13]
Nanowalls	thickness = 60~80nm, Length = 2~3um	Fingers bending	2.5V	80nA	200nW/cm^2	PET	[14]
Nanorods	Diameter = 50~170nm, Length = ~3um	Strain 0.5%	2.0V	15nA	75nW/cm^2	Terylene Fabrics	[15]
Nanowires	Length = ~2um	Mechanical strain	75mV	10nA		Ti Foil	[16]
Nanowires	Diameter = ~100nm	2Hz strained and released	2.1V (10 layers)	~105nA (10 layers)	~0.3mW/cm^2	Flexible substrate	[17]
Nanorods	Diameter = 30~80nm, Length = 1~1.5um	Cam bending	154mV	867μA/cm^2	36μW/cm^2	PET	[18]
Nanowires	Diameter = 100~200nm, Length = 2um	Respiration air flow	1.3V (16 fold)	0.8μA (16 fold)		PDMS (polydime-thylsiloxane)	[19]
Nanorods		Cam bending		4.76μA/cm^2		CNT/PES(polyester-rsulfone)	[20]
Nanorods	Diameter = 70~80nm, Length = ~1um	Loading 0.9kgf		10μA/cm^2		ITO/PES	[21]
Nanowires	Length = ~2um	Strain 0.12%	10V	0.6μA	10mW/cm^2	Polymide	[22]
V-doped nanosheets	thickness = 15~20nm, Length = 0.9~1um	Compressive strain		1.4μA/cm^2		ITO/PET	[23]
Nanowires	Diameter = 100nm, Length = 1um	Bending	300mV	16nA	4.8nW	Polymide	[24]
Ag-doped nanowires		Sound waves force	2V	0.5μA	0.5μW/cm^2	Polyster	[25]
Nanowires	Diameter = 500nm, Length = 7~8um	Strain 0.12%	8V	0.6μA	5.3mW/cm^3	PDMS (polydime-thylsiloxane)	[26]
Nanorods	Diameter = 100~200nm, Length = 4um	Strain (gasket height)	10mV	10nA		Paper	[27]
Nanowires	Length = 2um	wind	50mV	200nA		Al Foil	[28]
Nanowires+Pd nanparticles	Diameter = 200nm, Length = 5um	Strain 0.12%	0.52V			Ti Foil	[29]

18. J. Briscoe, N. Jalali, P. Woolliams, M. Stewart, P. M. Weaver, M. Cainb, S. Dunn, *Energy Environ. Sci.* 2013, **6**, 3035.
19. H. I Lin, D. S. Wuu, K. C. Shen, R. H. Horng, *ECS J. Solid State Sci. Technol.* 2013, **2**, P400.
20. D. Choi, M. Y. Choi, H. J. Shin, S. M. Yoon, J. S. Seo, J. Y. Choi, S. Y. Lee, J. M. Kim, S. W. Kim, *J. Phys. Chem. C*, 2010, **114**, 1379.
21. M. Y. Choi, D. Choi, M. J. Jin, I. Kim, S. H. Kim, J. Y. Choi, S. Y. Lee, J. M. Kim, S. W. Kim, *Adv. Mater.* 2009, **21**, 2185.
22. Y. F. Hu, Y. Zhang, C. Xu, L. Lin, R. L. Snyder, Z. L. Wang, *Nano Lett.* 2011, **11**, 2572.
23. M. K. Gupta, J. H. Lee, K. Y. Lee, S. W. Kim, *ACS Nano*, 2013, **7**, 8932.
24. T. S. van den Heever, W. J. Perold, *Microelectron. Eng.* 2013, **112**, 41.
25. S. Lee, J. Lee, W. Ko, S. Cha, J. Sohn, J. Kim, J. Park, Y. Park, J. Hong, *Nanoscale*, 2013, **5**, 9609.
26. L. Lin, Y. F. Hu, C. Xu, Y. Zhang, R. Zhang, X. N. Wen, Z. L. Wang, *Nano Energy*, 2013, **2**, 75.
27. Y. Qiu, H. Q. Zhang, L. Z. Hu, D. C. Yang, L. N. Wang, B. Wang, J. Y. Ji, G. Q. Liu, X. Liu, J. F. Lin, F. Li, S. J. Han, *Nanoscale*, 2012, **4**, 6568.
28. S. Lee, S. H. Bae, L. Lin, Y. Yang, C Park, S. W. Kim, S. N. Cha, H. Kim, Y. J. Park, Z. L. Wang, *Adv. Funct. Mater.* 2013, **23**, 2445.
29. Y. J. Lin, P. Deng, Y. X. Nie, Y. F. Hu, L. L. Xing, Y. Zhang, X. Y. Xue, *Nanoscale*, 2014, **6**, 4604.
30. C. L. Hsu, H. H. Li, T. J. Hsueh, *ACS Appl. Mater. Interfaces*, 2013, **5**, 11142.
31. C. L. Hsu, Y. D. Gao, Y. S. Chen, T. J. Hsueh, *ACS Appl. Mater. Interfaces*, 2014, **6**, 4277.
32. M.P. Lu, J. Song, M.Y. Lu, M.T. Chen, Y. Gao, L.J. Chen, Z.L. Wang, *Nano Lett.* 2009, **9**, 1223.
33. J. Liu, P Fei, J.H. Song, X.D. Wang, C.S. Lao, R. Tummala, Z.L. Wang, *Nano Lett.* 2008, **8**, 328.
34. T.T. Pham, K.Y. Lee, J.H. Lee, K.H. Kim, K.S. Shin, M.K. Gupta, B. Kumar, S.W. Kim, *Energy Environ. Sci.* 2013, **6**, 841.
35. Y.Q. Chen, X.J. Zheng, X. Feng, *Nanotechnology*, 2010, **21**, 055708.
36. G. Stan, C.V. Ciobanu, P.M. Parthangal, R.F. Cook, *Nano Lett.* 2007, **7,** 3691.
37. S. Xu, Y.G. Wei, J. Liu, R. Yang, Z.L. Wang, *Nano Lett.* 2008, **8**, 4027.
38. K.Y. Lee, B. Kumar, J.S. Seo, K.H. Kim, J.I. Sohn, S.N. Cha, D. Choi, Z.L. Wang, *Nano Lett.* 2012, **12**, 1959.